Science and Technology Indonesia
e-ISSN:2580-4391 p-ISSN:2580-4405
Vol. 9, No. 4, October 2024

Research Paper

Analysis of Structure, Morphology, Magnetic Properties, and Microwave Absorption of Lanthanum Orthoferrite ($LaFeO_3$)

Marzuki Naibaho[1,4], Januar Widakdo[1*], Budhy Kurniawan[1] Phahul Zhemas Zul Nehan[1], Okvarahireka Vitayaya[1], Novita[2], Ramlan[3], Wisnu Ari Adi[4], Masno Ginting[4*]

[1]Department of Physics, Universitas Indonesia, Depok, West Java, 16424, Indonesia
[2]Department of Physics, Universitas Sumatera Utara, Medan, North Sumatera, 20155, Indonesia
[3]Department of Physics, Faculty of Natural Sciences, Universitas Sriwijaya, Inderalaya, Ogan Ilir, South Sumatera, 30662, Indonesia
[4] Center for Advanced Materials Research (PRMM) - National Research and Innovation Agency (BRIN), Complex Puspiptek Building 440-441, Tangerang-South, Banten, 15314, Indonesia
*Corresponding author: Januar.widakdo@ui.ac.id, masn001@brin.go.id

Abstract
$LaFeO_3$ has been prepared using the solid-state reaction method with High Energy Milling (HEM). The preparation of $LaFeO_3$ was carried out using stoichiometric calculations. Based on the XRD measurement results, single-phase $LaFeO_3$ with an orthorhombic crystal structure was obtained. From the SEM results, the morphology of $LaFeO_3$ is uniform, and the EDS results show the weight percentage of La, Fe, and O elements are 49.74, 21.08, and 29.18 wt%, respectively. VSM $LaFeO_3$ results show magnetic saturation, remanence, and coercivity are 0.24 emu/g, 0.02 emu/g, and 853.38 Oe, respectively, and the absorption of $LaFeO_3$ is -7.40 dB at a frequency of 6.02 GHz with a $LaFeO_3$ sample thickness of 1.5mm.

Keywords
Perovskite, $LaFeO_3$, Morphology, Magnetic Properties, Microwave Absorption

Received: 15 May 2024, Accepted: 6 July 2024
https://doi.org/10.26554/sti.2024.9.4.851-856

1. INTRODUCTION

Magnetic materials are one of the classifications of advanced materials that contain a combination of iron oxide components or other metals to form new inorganic crystalline materials (Phahul Zhemas et al., 2024). This type of material is characterized by good permeability and permittivity values so that it can interact with complex electromagnetic waves (Deng, 2021). This magnetic material usually consists of a combination of rare earth metal elements and transition metals that produce magnetic properties that can function as an electromagnetic wave-absorbing material. Perovskite is one of the magnetic material candidates that has broad potential to be utilized in various applications in technology such as electromagnetic wave absorbing materials, sensor materials, etc (Meng et al., 2024; Wang et al., 2021).

Perovskite have the chemical formula as ABO_3. Site A has a large ionic radius, and site B has a small one. Rare earth metals have a large ionic radius size, so they are suitable for inclusion on site A. This is called rare earth perovskite. Ideally, ABO_3 compositions where (A is a rare earth metal cation and B is a 3d transition metal cation) such as the LFO system (Subudhi et al., 2020; Gomaa et al., 2022). Rare earth orthoferrites are the subject of recent research for beneficial applications in various electrode devices, solar cells, permanent magnet manufacturing, magnetic sensors, microwave absorbers, and many more (Makoed et al., 2020, 2022; Subudhi et al., 2020; Phahul Zhemas et al., 2024). These materials exhibit attractive magnetic and spin reorientation properties and ionic and electrical defects. In these materials, the small cation 'B' is at the center of the oxygen anion octahedron, and the large cation 'A' is at the corner of the unit cell (Azouzi et al., 2021; Saikia et al., 2022).

In the rare earth orthoferrite series, one of them, $LaFeO_3$ is of great interest to be discussed due to its various attractive features namely, a wide-gap antiferromagnetic insulator with high Néel temperature (TN~740°C), the coexistence of coupled ferroelectric and antiferromagnetic arrays, possessing good thermal properties and chemical properties(Acharya et al., 2010; Ateia et al., 2021). Previous research by Qiang Li and Guangzhou Zhu that $LaFeO_3$ material shows negative magnetic permeability at 2.6-2.8 GHz and negative permittivity at 0.8-1.2 GHz (Li and Zhu, 2021). The opposing magnetic permeability and permittivity allow this material to be used in

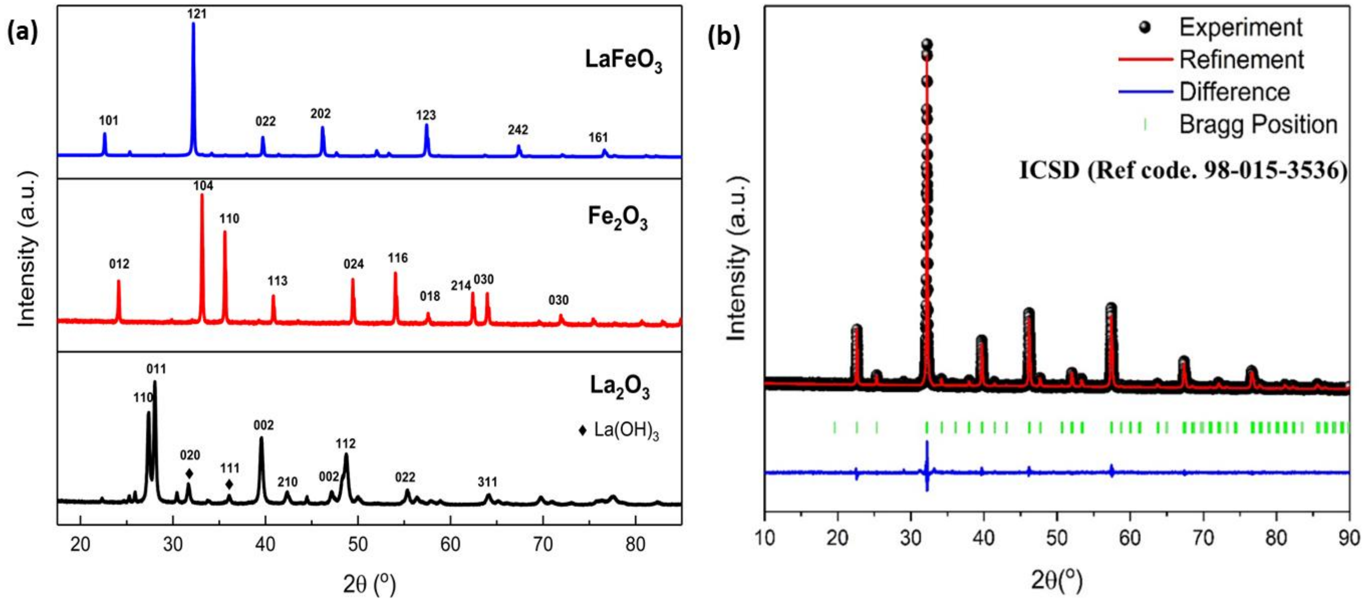

Figure 1. (a) Diffraction Patterns of La_2O_3, Fe_2O_3, and $LaFeO_3$, (b) Refinement Result of $LaFeO_3$

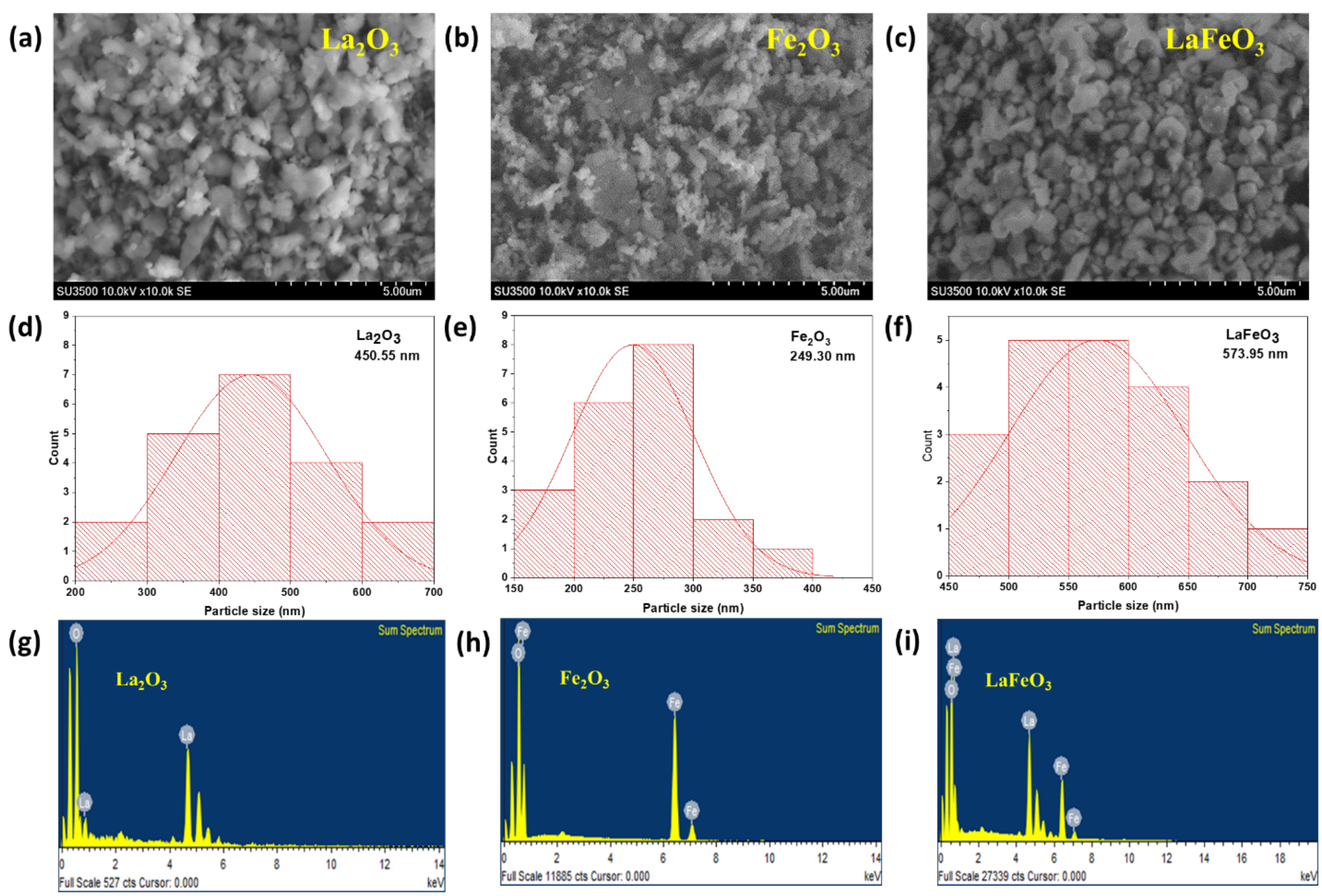

Figure 2. Morphology of (a) La_2O_3, (b) Fe_2O_3, and (c) $LaFeO_3$ with 10000 times magnification, particle size of (d) La_2O_3, (e) Fe_2O_3, and (f) $LaFeO_3$ and EDS results of (g) La_2O_3, (h) Fe_2O_3 and (i) $LaFeO_3$

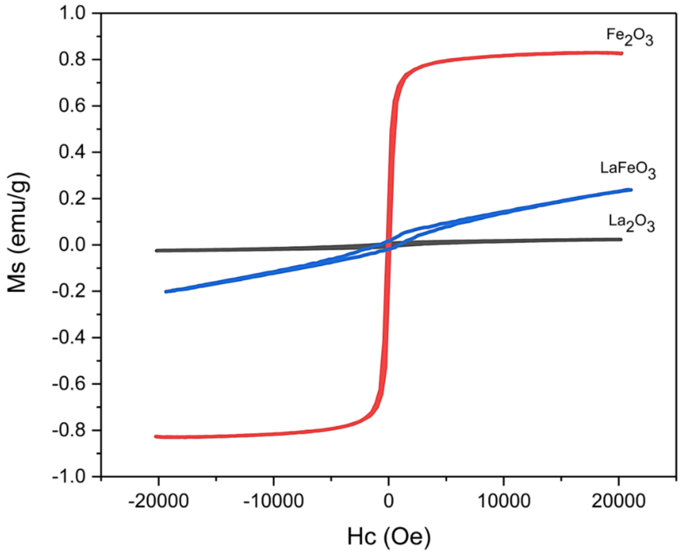

Figure 3. Hysteresis Curves of La_2O_3, La_2O_3 and $LaFeO_3$

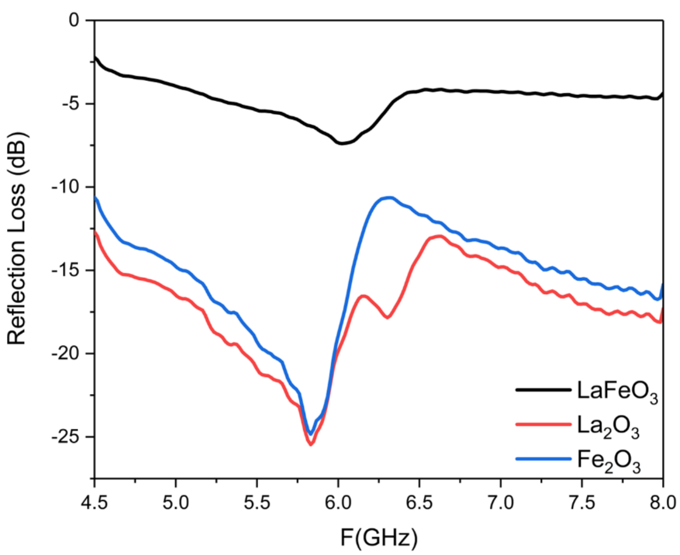

Figure 4. Reflection Loss Results of La_2O_3, La_2O_3 and $LaFeO_3$

the field of electromagnetic metamaterials. Based on previous research, $LaFeO_3$ has been prepared in various syntheses, such as the sol-gel method (Subudhi et al., 2020), Sol-gel auto combustion (Çoban Özkan et al., 2020), hydrothermal synthesis (Kayalvizhi et al., 2022), coprecipitation method (Rianna et al., 2023), electrospinning (Jeong et al., 2018), solid-state reaction method (Acharya et al., 2010; Mitra et al., 2018) and various other types of synthesized methods (Edianta et al., 2021; Elmahaishi et al., 2022; Pullar, 2012; Zhang et al., 2022).

This paper presents a comprehensive analysis of $LaFeO_3$ synthesized via the solid-state reaction method employing High Energy Milling (HEM). Our study aims to elucidate the structural, morphological, magnetic, and microwave absorption properties of $LaFeO_3$, contributing to a deeper understanding of its potential applications across various fields. Through meticulous characterization and analysis, we endeavor to shed light on the intricacies of $LaFeO_3$ and pave the way for its enhanced utilization in advanced technological applications.

2. EXPERIMENTAL SECTION

2.1 Materials

The materials used in this study were Lanthanum oxide (La_2O_3) of 99.9% purity and Hematite (α-Fe_2O_3) of 95% purity from LOBA CHEMIE PVT.LTD.

2.2 Methods

The materials used were weighed according to the stoichiometric calculation. The material was put into a vial with material-to-milling ball ratio of 1:5. In this works, the material used was 10 grams, and the ball was 50 grams. The material is then wet milled for 5 hours at 1000 m/s by adding ethanol. The sample dried in the oven for 20 hours at 85°C, then compressed at 4 tons pressure. Hence the sample is sintered for 5 hours at 1200°C. After sintering, the sample was crushed until 200 mesh sizes and then characterized using XRD (type SmartLab-Rigaku), SEM-EDX (type Hitachi SU3500), VSM (VSM250), and VNA (Advantest type R3770 300 kHz-20 GHz).

3. RESULTS AND DISCUSSION

Table 1. EDS Results of La_2O_3, Fe_2O_3 and $LaFeO_3$

Compound	Element Content (Wt%)		
	La	Fe	O
La_2O_3	61.27	-	38.73
Fe_2O_3	-	59.14	40.86
$LaFeO_3$	49.74	21.08	29.18

Table 2. Magnetic Saturation (Ms), Remanence (Mr), and Coercivity (Hc) of La_2O_3, Fe_2O_3, and $LaFeO_3$, Respectively

Name	Ms (emu/g)	Mr (emu/g)	Hc (Oe)
La_2O_3	0.06	0.04	867.14
Fe_2O_3	0.92	0.24	1.471
$LaFeO_3$	0.24	0.02	853.38

3.1 Analysis of Structure

The characterizations of synthesized nanomaterials have been done using XRD measurement. X-ray diffraction (XRD) analysis is a fundamental method for evaluating phase formation and crystallinity. The XRD patterns of oxide-based materials such as La_2O_3, α-Fe_2O_3, and $LaFeO_3$ are shown in Figure 1(a), and Figure 1(b) is a refinement of $LaFeO_3$. They were prepared by solid-state reaction using high energy milling (HEM).

Table 3. Structure and Magnetic Properties of $LaFeO_3$ in Previous Work

Method	Dsc (nm)	DSEM (nm)	Ms (emu/g)	Mr (emu/g)	Hc (Oe)	Reference
Solid state reaction mixed by agate mortar, 1400°C	24.3	NA	1.03	0.32	4030	(Mitra et al., 2018)
Sol-Gel Method, 600°C	30.4	NA	0.57	0.04	148.15	(Lin et al., 2018)
Sol-Gel Method, 1000°C	NA	NA	0.28	0.01	77.78	(Lin et al., 2018)
Sol-Gel Method, 500°C	26.57	846	0.81	0.15	123.41	(Çoban Özkan et al., 2020)
Sol-Gel Method, 850°C	29.69	439	0.57	0.06	79.13	(Çoban Özkan et al., 2020)
Co-Precipitation	24.6	39 - 77	6.5	0.5	1217.6	(Sasikala et al., 2017)
Co-precipitation	26.93	200	21.93	10.95	185.76	(Rianna et al., 2023)
Solid state reaction by High Energy Milling, 1200°C	24.23	573.95	0.24	0.02	853.38	This work

Table 4. Reflection Loss Parameters of La_2O_3, Fe_2O_3, and $LaFeO_3$

Name	Reflection Loss (dB)	F (GHz)
La_2O_3	-25.46	5.83
Fe_2O_3	-24.84	5.83
$LaFeO_3$	-7.40	6.02

Figure 1(a) shows the sample's X-ray diffraction pattern. In the crystallographic phase, Lanthanum Oxide (La_2O_3) has two compounds such as $La(OH)_3$ with peaks at (020), (111) and La2O3 with peaks including (110), (011), (002), (210), (002), (112), (022), (311). This is consistent and confirmed in ICSD (ref code. 98-0167480). The crystallographic phase of iron (II) oxide (Fe_2O_3) confirmed that all peaks belonged to Fe_2O_3 and no impurities were found, this is also by the data confirmed in ICSD (98-016-1283) and the strongest (100%) peak (121) of Fe_2O_3 was observed at 2θ = 33.147. When La_2O_3 and Fe_2O_3 materials are mixed using the solid-state reaction method with stoichiometric calculations, the $LaFeO_3$ phase is formed. The desired Lanthanum Orthoferrite $LaFeO_3$ crystallographic phase of the sample is confirmed by the ICSD file (Ref code. 98-015-3536) with space group Pnma (62) and has an Orthorhombic structure. All the peaks displayed in Figure 1 closely match $LaFeO_3$. No peaks except $LaFeO_3$ were detected in the XRD pattern, which can be confirmed in Figure 1(b). This results from $LaFeO_3$ refractoriness. The strongest (100%) peak (121) of $LaFeO_3$ was observed at 2θ = 32.196°.

3.2 Morphology and EDS Result

Figure 2 is the morphology and the elemental analysis of La_2O_3, Fe_2O_3, and $LaFeO_3$ observed using SEM (Scanning Electron Microscopy) and conducted by EDS (Energy Dispersive X-ray spectroscopy).

From Figure 2a-c on morphological observations using SEM carried out at a magnification of 10,000 times, in the image La_2O_3, Fe_2O_3 has a tiny particle size and forms agglomerates due to its small particle size. Meanwhile, in $LaFeO_3$, the particle size becomes more extensive. This occurs due to heating so that particles that were initially small experience nucleation, which forms a larger particle size or indicates the formation of a new phase (Liu et al., 2015).

From Figure 2d-f, the average particle size of La_2O_3, Fe_2O_3 and $LaFeO_3$ respectively are 450.55 nm, 249.30 nm, dan 573.95 nm. In Figure 2f it can be seen that the particle size is crystallized and enlarged due to the formation of new compounds from the precursor materials La_2O_3 and Fe_2O_3 into $LaFeO_3$. This has been confirmed by the XRD refinement results in Figure 1b.

From Figure 2g-i, the constituent components of each compound have no other elements or impurities. This can be seen in Table 1, where the weight of each element of each compound has no other elements present.

In Table 1 it can be seen that the La content in the La_2O_3 compound is by the stoichiometric calculations that have been made. Likewise with Fe in the Fe_2O_3 compound. So that when the La content dominates the formation of $LaFeO_3$ compared to Fe. This happens because the atomic weight of La is greater than Fe so in the weight ratio the element La is greater than Fe in the $LaFeO_3$ compound. This will also affect the magnetic properties of the $LaFeO_3$ compound which will be discussed in the next subchapter.

3.3 Magnetic Properties

The measurement results of the magnetic properties of La_2O_3, La_2O_3, and $LaFeO_3$, which were tested using VSM, can be seen in Figure 3.

From Figure 3, the hysteresis curves of La_2O_3, Fe_2O_3, and $LaFeO_3$ can be seen. The magnetic properties of $LaFeO_3$ have a minimal value of magnetic properties. This is because $LaFeO_3$ is known as weak ferromagnetic (FM) (Huang et al., 2022a). The magnetic structure of lanthanum orthoferrite has two intersecting pseudo-cubic face-centered sub-lattices consisting of FeO6 octahedral units. This indicates a collinear arrangement of the two sub-lattices, which gives it weak ferromagnetic properties (Huang et al., 2020; Huang et al., 2022a).

Nevertheless, the reduction in particle size led to a fun-

Table 5. The Amount of Microwave Absorption of $LaFeO_3$ that Has Been Done Before

Sample	Method	Reflection Loss	d(mm)	References
$LaFeO_3$	Sol-Gel	-10 dB (X-Band)	3.00	(Huang et al., 2022b)
$LaFeO_3$	Sol-Gel	-17.53 dB (Ku-Band)	1.8	(Huang et al., 2020)
$LaFeO_3$	Sol Gel	-12.20 dB (Ku-Band)	2.00	(Huang et al., 2022a)
$LaFeO_3$	Solid state reaction	- 7.40 dB (C-Band)	1.5	This work

damental change in the magnetic order across the particles. Namely, an uncompensated surface spin is generated by the increased surface area. More details of the magnetic properties can be seen in Table 2.

Table 2. Magnetic saturation (Ms), Remanence (Mr), and coercivity (Hc) of La_2O_3, Fe_2O_3, and$LaFeO_3$, respectively

In Table 2, it can be seen that La_2O_3 has a lower value of magnetic properties compared to Fe_2O_3. So, when La_2O_3 and Fe_2O_3 are combined with the solid-state reaction method, it will produce the$LaFeO_3$ compound.$LaFeO_3$ compounds have new magnetic properties that are between La_2O_3 and Fe_2O_3. This will also affect the amount of microwave absorption discussed in the next chapter.

In Table 3 is shown the Structure and magnetic properties of$LaFeO_3$ in previous work as the comparison to this work.

3.4 Microwave Absorption

The results of the microwave absorption of $LaFeO_3$ tested using VNA with the standard absorption performed at -10 dB can be seen in Figure 4.

Figure 4 shows the amount of microwave absorption or reflection loss on the$LaFeO_3$ sample with a sample thickness of 1.5 mm measured in the frequency range of 4.5-8 GHz (C-Band). The figure shows the optimum absorption value is -7.40 dB at a frequency of 6.02 GHz. This indicates that the microwave absorption capability has a low reflection loss, but on the bright side, it has a wide bandwidth, as shown in Table 4.

Some comparison of microwave absorption of$LaFeO_3$ material with several methods can be seen in Table 5.

This$LaFeO_3$ material has a bandwidth value, so it is promising to be used as a candidate for microwave-absorbing materials (MAMs). However, because the reflection loss value is still not deep enough, it is necessary to modify the structure to be used as a MAM material. One way is to substitute rare earth metals such as Nd, Gd, and Dy for La or other transition metals such as Mn, Co, and Ni for Fe in the Orthoferrite system.

4. CONCLUSION

In this study, we successfully made$LaFeO_3$ material using a solid-state reaction method using high energy milling (HEM). Based on the XRD data, it was found that the single-phase$LaFeO_3$ and no other phases were found, and this was corroborated based on the refinement results. SEM-EDS results found no elements other than La, Fe, and O. VSM results show that$LaFeO_3$ is antiferromagnetic and tested at room temperature. The VNA obtained optimum results on the amount of absorption of -7.40 dB at 6.02 GHz with a thickness of 1.5mm. Research on perovskite materials still has the potential for further study. Therefore, developing or modifying$LaFeO_3$ material as a microwave-absorbing material is essential. Because this$LaFeO_3$ material has a broad bandwidth value, it is promising to be used as a candidate for microwave-absorbing materials (MAMs). However, because the reflection loss (RL) value is still not deep enough, it is necessary to modify the structure to be used as an MAM material.

5. ACKNOWLEDGMENT

This research was supported by a degree by research scholarship, and this research was facilitated by the magnetic material preparation laboratory of the Center for Advanced Materials Research - National Research and Innovation Agency (PRMM-BRIN). This research is funded by Directorate of Research and Development, Universitas Indonesia under Hibah PUTI Pascasarjana 2024 (Grant No. NKB-110/UN2.RST/HKP.05.00/-2024).

REFERENCES

Acharya, S., J. Mondal, S. Ghosh, S. K. Roy, and P. K. Chakrabarti (2010). Multiferroic Behavior of Lanthanum Orthoferrite ($LaFeO_3$). *Materials Letters*, **64**(3); 415–418

Ateia, E. E., H. Ismail, H. Elshimy, and M. K. Abdelmaksoud (2021). Structural and Magnetic Tuning of $LaFeO_3$ Orthoferrite Substituted Different Rare Earth Elements to Optimize Their Technological Applications. *Journal of Inorganic and Organometallic Polymers and Materials*, **31**(4); 1713–1725

Azouzi, W., I. Benabdallah, A. Sibari, H. Labrim, and M. Benaissa (2021). Structural and Optical Properties of $LaFe_{1-x}V_xO_3$ as Predicted by a DFT Study. *Materials Today Communications*, **26**; 3–9

Çoban Özkan, D., A. Türk, and E. Çelik (2020). Synthesis and Characterizations of Sol–Gel Derived $LaFeO_3$ Perovskite Powders. *Journal of Materials Science: Materials in Electronics*, **31**(24); 22789–22809

Deng, J. (2021). Microwave Absorbing Properties of $La_{1-x}Ba_xMnO_3$(x=0.1,0.2,0.3,0.4,0.5) Nano-Particles. *Journal of Physics: Conference Series*, **1777**(1); 5–10

Edianta, J., N. Fauzi, M. Naibaho, F. S. Arsyad, and I. Royani (2021). Review of the Effectiveness of Plant Media Extracts in Barium Hexaferrite Magnets ($Bafe_{12}O_{19}$). *Science and Technology Indonesia*, **6**(2); 39–52

Elmahaishi, M. F., R. S. Azis, I. Ismail, and F. D. Muhammad (2022). A Review on Electromagnetic Microwave Absorption Properties: Their Materials and Performance. *Journal of Materials Research and Technology*, **20**; 2188–2220

Gomaa, M. M., M. H. Sayed, A. M. Abo El-Soud, and M. Boshta (2022). The Influence of K Substitution on the Structural, Optical and Magnetic Properties of $LaFeO_3$ Perovskites. *Solid State Communications*, **342**; 114615

Huang, L., L. Cheng, S. Pan, Y. He, C. Tian, J. Yu, and H. Zhou (2020). Effects of Sr Doping on the Structure, Magnetic Properties and Microwave Absorption Properties of $LaFeO_3$ Nanoparticles. *Ceramics International*, **46**(17); 27352–27361

Huang, L., L. Cheng, S. Pan, Q. Yao, Q. Long, M. Wang, Y. Chen, and H. Zhou (2022a). Influence of A-Site Doping Barium on Structure, Magnetic and Microwave Absorption Properties of $LaFeO_3$ Ceramics Powders. *Journal of Rare Earths*, **40**(7); 1106–1117

Huang, L., M. Wang, L. Cheng, S. Pan, Q. Yao, and H. Zhou (2022b). Fast and Efficient Synthesis of a New Adjustable Perovskite-Structured Ferrite $La_{1-x}Ca_xFeO_3$ Microwave Absorbent. *Journal of Alloys and Compounds*, **892**; 162167

Jeong, J. H., C. G. Song, K. H. Kim, W. Sigmund, and J. W. Yoon (2018). Effect of Mn Doping on Particulate Size and Magnetic Properties of $LaFeO_3$ Nanofiber Synthesized by Electrospinning. *Journal of Alloys and Compounds*, **749**; 599–604

Kayalvizhi, T., A. Sathya, and K. R. S. Preethi Meher (2022). Hydrothermal Synthesis of Perovskite $CsPbBr_3$: Spotlight on the Role of Stoichiometry in Phase Formation Mechanism. *Journal of Electronic Materials*, **51**(7); 3466–3475

Li, Q. and G. Zhu (2021). Controlling Negative Permittivity and Permeability Behavior in $LaFeO_3$ through Sintering Temperature. *Ceramics International*, **47**(4); 5244–5248

Lin, Q., X. Yang, J. Lin, Z. Guo, and Y. He (2018). The Structure and Magnetic Properties of Magnesium-Substituted $LaFeO_3$ Perovskite Negative Electrode Material by Citrate Sol-Gel. *International Journal of Hydrogen Energy*, **43**(28); 12720–12729

Liu, L., A. Han, M. Ye, and M. Zhao (2015). Synthesis and Characterization of Al^{3+} Doped $LaFeO_3$ Compounds: A Novel Inorganic Pigments with High Near-Infrared Reflectance. *Solar Energy Materials and Solar Cells*, **132**; 377–384

Makoed, I. I., N. A. Liedienov, A. V. Pashchenko, G. G. Levchenko, D. D. Tatarchuk, Y. V. Didenko, A. A. Amirov, G. S. Rimski, and K. I. Yanushkevich (2020). Influence of Rare-Earth Doping on the Structural and Dielectric Properties of Orthoferrite $La_{0.50}R_{0.50}FeO_3$ Ceramics Synthesized Under High Pressure. *Journal of Alloys and Compounds*, **842**; 155859

Makoed, I. I., N. A. Liedienov, H. Zhao, Z. Ding, G. G. Levchenko, A. A. Amirov, G. S. Rymski, A. M. Zhivulko, and K. I. Yanushkevich (2022). Influence of Rare-Earth Doping on the Structural and Magnetic Properties of Orthoferrite $La0.50R0.50FeO_3$ Ceramics Obtained Under High Pressure. *Journal of Physics and Chemistry of Solids*, **170**; 110926

Meng, F., L. Qin, H. Gao, H. Zhu, and Z. Yuan (2024). Perovskite-Structured LaFeO3 Modified $In2O_3$ Gas Sensor with High Selectivity and Ultra-Low Detection Limit for 2-Butanone. *Journal of Alloys and Compounds*, **970**; 172464

Mitra, A., A. S. Mahapatra, A. Mallick, A. Shaw, N. Bhakta, and P. K. Chakrabarti (2018). Improved Magneto-Electric Properties of $LaFeO_3$ in $La_{0.8}Gd_{0.2}Fe_{0.97}Nb_{0.03}O_3$. *Ceramics International*, **44**(4); 4442–4449

Phahul Zhemas, Z. N., O. Vitayaya, D. R. Munazat, M. T. E. Manawan, D. Darminto, and B. Kurniawan (2024). The Magnetocaloric Effect Properties For Potential Applications Of Magnetic Refrigerator Technology: A Review. *Physical Chemistry Chemical Physics*, **26**(20); 14476–14504

Pullar, R. C. (2012). Hexagonal Ferrites: A Review of the Synthesis, Properties and Applications of Hexaferrite Ceramics. *Progress in Materials Science*, **57**(7); 1191–1334

Rianna, M., T. Sembiring, E. Amiruddin, and P. Sebayang (2023). Co-Precipitation Synthesis of $LaFe1-xAlxO_3$ (x = 0–0.2) on Structure and Electromagnetic Properties. *Materials Science for Energy Technologies*, **6**; 43–47

Saikia, N., R. Chakravarty, S. Bhattacharjee, R. L. Hota, R. K. Parida, and B. N. Parida (2022). Synthesis and Characterization of Gd-Doped $LaFeO_3$ for Device Application. *Materials Science in Semiconductor Processing*, **151**; 106969

Sasikala, C., N. Durairaj, I. Baskaran, B. Sathyaseelan, M. Henini, and E. Manikandan (2017). Transition Metal Titanium (Ti) Doped $LaFeO_3$ Nanoparticles for Enhanced Optical Structural and Magnetic Properties. *Journal of Alloys and Compounds*, **712**; 870–877

Subudhi, S., A. Mahapatra, M. Mandal, S. Das, K. Sa, I. Alam, B. V. R. S. Subramanyam, J. Raiguru, and P. Mahanandia (2020). Effect of Co Doping in Tuning the Band Gap of $LaFeO_3$. *Integrated Ferroelectrics*, **205**(1); 61–65

Wang, M., L. Cheng, L. Huang, S. Pan, Q. Yao, C. Hu, Q. Liang, and H. Zhou (2021). Effect of Sr Doped the $YFeO_3$ Rare Earth Ortho-Ferrite on Structure, Magnetic Properties, and Microwave Absorption Performance. *Ceramics International*, **47**(24); 34159–34169

Zhang, S., Z. Jia, B. Cheng, Z. Zhao, F. Lu, and G. Wu (2022). Recent Progress of Perovskite Oxides and Their Hybrids for Electromagnetic Wave Absorption: A Mini-Review. *Advanced Composites and Hybrid Materials*, **5**(3); 2440–2460

